NEOPLASIA
www.neoplasia.com

Volume 10 Number 11 November 2008 pp. 1268–1274 1268

Chemotherapy-Induced Apoptosis in a Transgenic Model of Neuroblastoma Proceeds Through *p53* Induction[1,2]

Louis Chesler[*,†,‡], David D. Goldenberg[§], Rodney Collins[¶], Matt Grimmer[*], Grace E. Kim[¶], Tarik Tihan[¶], Kim Nguyen[§], Slava Yakovenko[§], Katherine K. Matthay[*] and William A. Weiss[*,†,§,#]

[*]Department of Pediatrics, University of California, San Francisco, San Francisco, CA 94143, USA; [†]Diller Family Comprehensive Cancer Center, University of California, San Francisco, San Francisco, CA 94143, USA; [‡]Paediatric Oncology Group, The Institute of Cancer Research, Sutton, Surrey, SM2 5NG, UK; [§]Department of Neurology, University of California, San Francisco, San Francisco, CA 94143, USA; [¶]Department of Pathology, University of California, San Francisco, San Francisco, CA 94143, USA; [#]Department of Neurological Surgery and The Brain Tumor Research Center, University of California, San Francisco, San Francisco, CA 94143, USA

Abstract

Chemoresistance in neuroblastoma is a significant issue complicating treatment of this common pediatric solid tumor. *MYCN*-amplified neuroblastomas are infrequently mutated at p53 and are chemosensitive at diagnosis but acquire *p53* mutations and chemoresistance with relapse. Paradoxically, Myc-driven transformation is thought to require apoptotic blockade. We used the TH-*MYCN* transgenic murine model to examine the role of p53-driven apoptosis on neuroblastoma tumorigenesis and the response to chemotherapy. Tumors formed with high penetrance and low latency in *p53*-haploinsufficient TH-*MYCN* mice. Cyclophosphamide (CPM) induced a complete remission in *p53* wild type TH-*MYCN* tumors, mirroring the sensitivity of childhood neuroblastoma to this agent. Treated tumors showed a prominent proliferation block, induction of p53 protein, and massive apoptosis proceeding through induction of the Bcl-2 homology domain-3–only proteins PUMA and Bim, leading to the activation of Bax and cleavage of caspase-3 and -9. Apoptosis induced by CPM was reduced in *p53*-haploinsufficient tumors. Treatment of MYCN-expressing human neuroblastoma cell lines with CPM induced apoptosis that was suppressible by siRNA to p53. Taken together, the results indicate that the p53 pathway plays a significant role in opposing *MYCN*-driven oncogenesis in a mouse model of neuroblastoma and that basal inactivation of the pathway is achieved in progressing tumors. This, in part, explains the striking sensitivity of such tumors to chemotoxic agents that induce p53-dependent apoptosis and is consistent with clinical observations that therapy-associated mutations in *p53* are a likely contributor to the biology of tumors at relapse and secondarily mediate resistance to therapy.

Neoplasia (2008) 10, 1268–1274

Address all correspondence to: Louis Chesler, MD, PhD, The Institute of Cancer Research, 15 Cotswold Rd. Belmont, Sutton, Surrey, SM2 5NG, UK.
E-mail: louis.chesler@icr.ac.uk

[1]Grant numbers and sources of support: National Institutes of Health (grants R01CA102321 (W.A.W.), K08NS053530 (L.C.), the Thrasher Research Fund (W.A.W.) and the Samuel Waxman Cancer Research Foundation (W.A.W.), The Katie Dougherty Foundation (W.A.W.), the Children's Neuroblastoma Cancer Foundation (L.C.), the Campini Family Foundation (L.C.), and the UK Neuroblastoma Society (L.C.).
[2]This article refers to supplementary materials, which are designated by Figures W1 to W4 and are available online at www.neoplasia.com.
Received 11 July 2008; Revised 13 August 2008; Accepted 14 August 2008

DOI 10.1593/neo.08778

Introduction

Neuroblastoma is the most common extracranial solid tumor of childhood [1]. The proto-oncogene *MYCN* is amplified in one third of neuroblastomas and is associated with high-risk disease and poor survival [1–5]. The ability of Myc proteins to induce malignant transformation is limited by coordinate induction of both proliferation and apoptosis [6–8]. Consequently, mutations of p53 are common in several Myc-driven malignancies at diagnosis and enhance oncogenesis.

In neuroblastoma, genetic defects in the p53 pathway function (mutation in *p53* or $p14^{ARF}$, amplification of *MDM2*) are rare at diagnosis but are present in cell lines established from patients treated with prolonged therapy [9–12]. In the absence of such mutations, amplification of *MYCN* in newly diagnosed neuroblastomas is typically associated with epigenetic abnormalities that impair apoptosis: silencing of caspase-8 or overexpression of the antiapoptotic proteins Bcl-2 and survivin [13–15]. These events are independently associated with poor outcome in neuroblastoma and represent potential mechanisms contributing to malignant progression [13,15,16].

Despite such defects in apoptotic signaling, newly diagnosed neuroblastoma tumors typically respond to chemotherapeutics such as cyclophosphamide (CPM) irrespective of risk group, suggesting that epigenetic regulation of apoptotic pathways is either insufficient to block apoptosis in response to cytotoxic chemotherapy or is not initially present at diagnosis [17,18]. Because virtually all patients respond to initial therapy, outcome in this disease is mainly determined by the likelihood of relapse, with high-risk patients (including tumors that show amplification of *MYCN*) frequently relapsing with drug-resistant tumors [10,19].

The TH-*MYCN* model shows that coordinate mutation of *p53* is not required for *MYCN*-driven oncogenesis in neuroblastoma, mirroring the situation in human high-risk tumors. It follows that apoptosis is functionally suppressed by other means. However, this presents a paradox in that *MYCN*-driven murine neuroblastomas retain exquisite sensitivity to chemotherapeutics, which exert their effects through induction of apoptosis. To examine this question, we sought to determine whether the p53 pathway was active or inactive in TH-*MYCN* and whether induction of the pathway occurred in response to chemotherapy.

TH-*MYCN* is a native neuroblastoma model in which tumorigenesis is driven by targeted expression of a TH-*MYCN* transgene in the neural crest of transgenic mice [20]. These animals develop an aggressive malignancy that is morphologically, genetically, and clinically similar to human high-risk *MYCN*-amplified neuroblastoma [21,22]. We show that *p53* haploinsufficiency enhances the effect of *MYCN*-driven transformation in neuroblastoma, that basal p53 pathway function and apoptosis are suppressed in such tumors (in contrast to *in vitro* observations), that haploinsufficiency amplifies the effect of MYCN on transformation in neuroblastoma, and that the chemoresponse of effective agents such as CPM requires intact p53-driven apoptosis. Mechanistically, CPM induces p53 and activates a variety of p53 targets critical to apoptosis, including PUMA, Bim, Bax, caspase-3, caspase-9, and poly(ADP-ribose) polymerase (PARP). The *in vivo* response of TH-*MYCN*–driven tumors to CPM is similar to that observed in cultured human cell lines treated with CPM. In three cell lines with equivalent levels of p53 protein but increasing levels of Mycn, the apoptotic response to CPM correlated with the induction of p53 and could be blocked by siRNA to p53.

Taken together, these data document the activity in murine tumors of a frontline chemotherapeutic agent used in children with newly diagnosed neuroblastoma and add to evidence validating mice transgenic for TH-*MYCN* as a preclinical platform for developmental therapeutics. Furthermore, these observations highlight the utility of mice transgenic for TH-*MYCN* as a preclinical model in which to delineate the kinetics and details of apoptotic signaling in response to CPM. The induction and functional activation of p53 in these tumors reinforce the importance of p53 signaling in the therapeutic response to cytotoxic chemotherapy. These observations are also consistent with clinical data that cytotoxic chemotherapy selects for loss of p53 function, that recurrence in neuroblastoma is subsequently driven by *p53* mutation, and that *p53* mutation in relapsed tumors contributes secondarily to therapeutic resistance [10,23,24].

Materials and Methods

Cell Culture and Treatments

SHEP, SK-N-SH, SH-SY5Y, and Kelly neuroblastoma cell lines were obtained from the University of California at San Francisco. Cells were grown in Dulbecco's modified Eagle's medium with 10% FBS at 37°C. 4-Hydroxyperocyclophosphamide (4^{OH}-CPM) was obtained from Susan Ludeman (University of North Carolina) and was dissolved at 20 mg/ml in water. For *in vivo* therapy, CPM from the University of California at San Francisco Clinical Pharmacy was dissolved at 1 mg/ml.

Proliferation and Apoptosis Assays

Cell growth and proliferation were assessed by soluble tetrazolium (WST-1; Roche, Indianapolis, IN). Necrosis and apoptosis were assessed using a Cell Death Detection ELISA (Roche) that detects intracellular or released nucleosomal $H2_b$ DNA. Values were corrected for vehicle (DMSO). Cells were plated and assayed at 6 to 24 hours using a Synergy HT-1 spectrophotometer (Biotek, Winooski, VT). Percent toxicity was standardized using Triton X-100 as a positive control (0-100 mM).

Immunoblot Analysis and Antibodies

Cells were suspended in nondenaturing lysis buffer (Cell Signaling Technology, Danvers, MA) with 0.5% SDS. Lysates were sonicated and cleared at 14,000*g* at 4°C. Protein content was assayed by the BCA method (Pierce, Rockford, IL), and 20 to 40 μg of protein was analyzed on 4% to 12% gradient denaturing gels (Invitrogen, Carlsbad, CA). Membranes were incubated overnight at 4°C with primary antibodies [cleaved caspase-3 (9664; Cell Signaling Technology), caspase-9 (9508; Cell Signaling Technology), p53 (9282; Cell Signaling Technology), Bim (4582; Cell Signaling Technology), Bax (2772; Cell Signaling Technology), PARP (9542; Cell Signaling Technology), PUMA (4976; Cell Signaling Technology), and β-tubulin (05-661; Upstate, Billerica, MA)] and visualized using HRP-conjugated secondary antibodies (Calbiochem, Gibbstown, NJ) and ECL-Plus reagents.

Immunohistochemistry

For frozen sections, mice were killed after therapy, and tumors were embedded in Tissue-Tex O.C.T. compound (Sakura, Torrance, CA), cooled at −80°C (24 hours), sectioned at 4-μm thickness, mounted on Superfrost slides (Fisher Scientific, Pittsburgh, PA), and placed in 70% ethanol (1 hour at 4°C). Slides were washed three times with wash buffer (Dako, Carpinteria, CA), treated with 3% hydrogen peroxide (for 10 minutes), rewashed, blocked with casein (for 10 minutes), and incubated with caspase-3 antibody

(CST 9664) at a dilution of 1:100 at room temperature in a humidified chamber (for 2 hours). Slides were rewashed three times and incubated with rabbit Envision$^+$ secondary antibody (Dako) at room temperature in a humidified chamber (for 30 minutes) treated with Dako DAB$^+$ complex (for 4 minutes), rinsed with water, counterstained with Gills modified hematoxylin (American Master Tech, Lodi, CA), dehydrated, and mounted for analysis. Paraffin-embedded tissues were cut and mounted, deparaffinized with xylene through graded alcohol to water, and then placed in PBS. Heat-induced epitope retrieval was performed at 120°C in citrate buffer at pH 6.0, followed by treatment in 3% peroxide (for 20 minutes). Washing and antibody incubations were as previously mentioned. Ki-67 staining in paraffinized sections was performed using a Ki-67 rat primary antibody (M7249; Dako) in a 3-hour incubation followed by processing as previously mentioned. Development was with streptavidin HRP (Amersham, Piscataway, NJ) at a dilution of 1:100 for 1 hour at room temperature.

In Vivo *Therapy in TH*-MYCN *Transgenic Mice*

TH-*MYCN* mice were maintained in hemizygotic matings as previously described [20]. Hemizygous TH-*MYCN* were serially crossed to p53+/– mice (FVBN) [25] and E_2F_1-luciferase mice (FVBN) [26] for more than four generations to re-establish tumor penetrance in the 129X1/SvJ strain. A similar approach was used in luciferase crosses. For the analysis of the *in vivo* effects of CPM on tumor growth in mice transgenic for TH-*MYCN* (in strain 129X1/SvJ), a tumor intervention design was implemented. The assay end point was tumor mass. In parallel experiments, tumor response and progression were confirmed using luciferase bioimaging of TH-*MYCN*/E_2F_1-Luc doubly transgenic animals, in which a luciferase signal is emitted from proliferating tumor tissue and is a surrogate indicator of Mycn activity. Animals (seven per arm) with palpable tumors (approximately 60 days of life) were treated three times per week with intraperitoneal injections of CPM (150 mg/kg in 100 μl of saline) or vehicle (saline) and were then killed. In parallel, animals (three per arm) were followed by noninvasive imaging, using the Xenogen IVIS Lumina system (Caliper Life Sciences, Hopkinton, MA) with a background bioluminescence setting of 38,000 photons/sec per square centimeters. At sacrifice, tumors were imaged, excised, measured, weighed, and snap-frozen for further analysis. Lysates were prepared for immunoblot analysis as previously mentioned, except that tumors were initially homogenized in TBS with protease inhibitors (Compleat; Roche, Inc.) before lysis. Significance analysis was performed using the Student's *t* test. All animals were handled in accordance with institutional guidelines for safe and ethical treatment of mice.

Results

Effect of p53 Heterozygosity on Neuroblastoma Tumor Formation in Mice Transgenic for TH-MYCN

Given the critical role of p53 in regulating myc-driven oncogenesis, we sought to evaluate induction of apoptosis by p53 in spontaneously growing neuroblastoma tumors originating within a native murine background. We therefore used the well-characterized TH-*MYCN* neuroblastoma model in which tyrosine hydroxylase (TH)–mediated overexpression of MYCN is targeted to the peripheral neural crest [20]. This model faithfully recapitulates high-risk human neuroblastoma tumorigenesis by all major clinicopathologic criteria. To evaluate the effect of p53 dysfunction on TH-*MYCN*–driven neuroblastoma tumor formation, we introduced TH-*MYCN* into a p53-deficient background by serial crosses against animals with an inactivated germ line *p53* allele [25]. Tumors arose in doubly transgenic animals with higher penetrance and reduced latency (Figure 1*A*). The initial anatomic appearance of these tumors was similar to that of p53 wild type TH-*MYCN* tumors (Figure 1*B*), but end-stage tumors were larger and were characterized by a higher density of proliferating neuroblasts and lower levels of apoptosis and necrosis on histologic analysis (Figure 1, *C* and *D*). Taken together, the data imply that, in neuroblastoma tumor progression, inactivation of p53 could enhance *MYCN* oncogenicity, at least in part by decoupling the growth-stimulatory activity of *MYCN* from its ability to concurrently drive apoptosis.

Cyclophosphamide Induces Durable Remissions in Mice Transgenic for TH-MYCN

Because intact p53 function inhibits growth and progression of TH-*MYCN* neuroblastoma tumors, we used CPM to assess whether established murine TH-*MYCN* tumors are sensitive to chemotherapeutics that exert their activity at least in part through p53 up-regulation. Cyclophosphamide induced complete regression of established tumors, with a dramatic effect on survival intervals (cumulative tumor free days

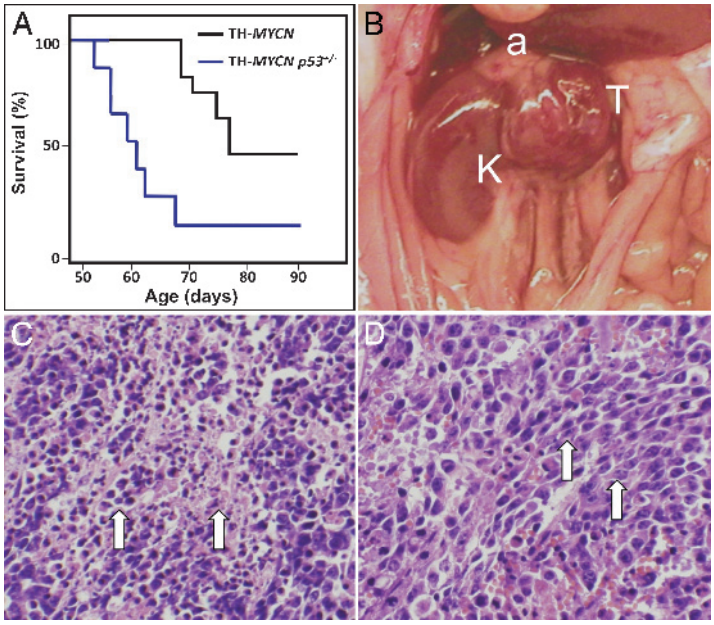

Figure 1. p53 heterozygosity enhances tumorigenesis in TH-*MYCN* neuroblastoma. TH-*MYCN* mice were introduced into a p53+/– background by sequential breeding against p53+/– FVBN animals, and cohorts of mice were followed for tumor formation. (A) Kaplan-Meier survival analysis of animal cohorts showing increased tumor penetrance (85% in p53+/–, 60% in p53+/+ animals) and shorter time to tumor onset (70 days of life in p53+/+, 50 days of life in p53+/–). (B) Early-stage focal tumor (T) of adrenal origin (a) on the superior pole of the kidney (K). (C, D) Histologic appearance of representative, large, late-stage p53+/+ and p53+/– TH-*MYCN* tumors showing a reduction of apoptotic cells with hyperchromatic nuclei on pale backgrounds and necrotic cells with pyknotic nuclei with hyaline staining (white arrows) in p53+/– tumor (D) *versus* p53+/+ tumor (C), white arrows. The p53+/– tumor is also relatively more monomorphous with densely packed neuroblasts (white arrows).

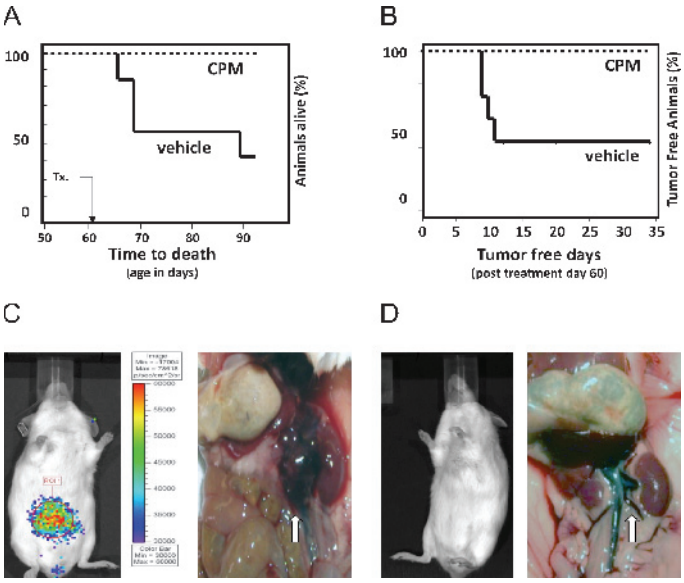

Figure 2. CPM induces durable remission in mice transgenic for TH-*MYCN*. Cohorts of transgene-positive animals (seven per arm) were randomly assigned to receive treatment with either control (saline) or CPM (150 mg/kg per day injected intraperitoneally three times per week). Animals were treated at approximately 60 days of life, when tumors were palpable. (A) Survival after treatment (day of life, 60). All treated animals survived to >100 days of life. Saline-treated animals required euthanasia owing to signs of advanced disease at or before 90 days of life. (B) Tumor-free survival after treatment on day of life 60. All CPM-treated animals remained tumor-free, whereas saline-treated animals developed tumors 10 days after treatment (70 days of life). The proportion of saline-treated animals remaining tumor-free is shown on the *Y* axis, plotted against tumor-free days after treatment on the *X* axis. (C) At treatment initiation, animals harbored focal tumors (white arrow), with strong E_2F_1-driven luciferase bioluminescence of up to 6×10^5 photons/sec per square centimeters. At autopsy, animals in the control group harbored large tumors (not shown). (D) No tumors or luciferase bioluminescence were detected in treated animals at 100 days of life (white dashed outline).

of life; Figure 2*A*) and time to death from overwhelming tumor burden (Figure 2*B*). Tumors in the control cohort were readily apparent on necropsy and by luciferase bioimaging of parallel animals doubly transgenic for TH-*MYCN* and E_2F_1-luciferase (representative animal shown in Figure 2*C*). Seven CPM-treated animals were killed at 100 days of life, with no evidence of tumor on necropsy and negative luciferase signals (representative animal shown in Figure 2*D*). These data show that tumors in TH-*MYCN* transgenic mice are sensitive to CPM, mirroring similar observations in *MYCN*-amplified human neuroblastoma.

Cyclophosphamide Inhibits Tumor Proliferation and Stimulates Apoptosis In Vivo

To analyze the effect of CPM on apoptosis, necrosis, and proliferation, we treated a cohort of transgenic animals with early, established tumors, sacrificing animals at several time points within 24 hours of CPM treatment. Tumors showed no changes in vascularity (data not shown) and exhibited no obvious cellular or structural changes (observable apoptosis or necrosis) in response to CPM treatment (Figure W1, *A–C*). In vehicle-treated tumors, immunoreactivity for the proliferation marker Ki-67 was positive in most nuclei (Figure 3, *A* and *B*). In response to CPM, Ki-67 labeling decreased dramatically even by 24 hours (Figure 3*C*). Whereas control tumors had negligible staining for the apoptosis marker cleaved caspase-3 (Figure 3*D*), high levels of cleaved caspase-3 were observed 3 and 6 hours after treatment with CPM (Figure 3, *E* and *F*). A wave of apoptosis throughout the tumor was demonstrated at low power (Figure 3, *H–J*), with maximal staining visible at 6 hours after treatment. At 24 hours, apoptotic staining was associated with foci of necrosis (Figure 3*J*, *inset*). Significantly, levels of apoptosis induced by similar treatment of *p53*-haplodeficient tumors with CPM were minimal, as assessed by immunostaining for cleaved caspase-3 (Figure W2). No significant differences in apoptosis were seen by immunohistologic analysis in vehicle-treated p53+/– *versus* p53+/+ tumors (data not shown).

Apoptosis in Tumors Treated with Cytotoxic Chemotherapy Is Driven by p53

To evaluate apoptotic signaling in response to CPM, we treated a cohort of early tumor-bearing transgenic animals and assessed levels of key apoptotic proteins by immunoblot (Figure 4*A*). In contrast to basal apoptotic activity detectable by immunoblot analysis of cultured neuroblastoma cell lines, activation of the p53 pathway and caspase-3 cleavage were minimal in vehicle-treated tumors, consistent with the low-level caspase-3 staining seen in Figure 4. Rapid induction of p53 was observed at 3 hours after treatment with CPM, with a peak at 6 hours after treatment (Figure 4*A*). Cleaved caspase-3 and -9 were maximal at 6 hours after treatment and were sustained during a 12-hour period. These data indicate that basal apoptotic activity in spontaneously progressing TH-*MYCN* neuroblastomas is minimal but that p53-driven apoptosis is intact and can be strongly induced in response to cytotoxic chemotherapy.

CPM Treatment of Murine Neuroblastoma Activates Apoptosis

PUMA and Bim are Bcl-2 homology 3 (BH3)–only proteins, proapoptotic components of the mitochondrial cell death pathway, and are critical effectors of p53-induced apoptosis in Myc protein–driven tumors [27]. In response to CPM treatment, PUMA was strongly induced *in vivo*, peaking at 3 hours and dissipating by 12 hours (Figure 4*A*). Bax, a downstream target of PUMA and a critical effector of myc-induced mitochondrial apoptosis, was strongly expressed (Figure 4*B*). Bim, a BH3-only protein necessary for apoptosis in myc-driven lymphoma, was induced prominently. Cleavage of caspases-3 and -9 (Figure 4*A*) and PARP (Figure 4*B*) occurred concurrently, indicating high levels of apoptosis. Taken together, these findings indicate that the proapoptotic effect of CPM proceeds through the intrinsic p53 regulatory pathway of BH3 proteins, implicating PUMA, Bax, and Bim as key effectors of p53 function in primary murine neuroblastoma tumors.

CPM Induces p53-Dependent Apoptosis in Human MYCN-*Amplified Neuroblastoma Cell Lines*

To determine whether levels of Mycn influence response to CPM in human tumors, we examined a panel of human neuroblastoma cell lines in which levels of Mycn were undetectable (SH-EP), intermediate (SH-SY5Y), or high (Kelly). All lines expressed roughly comparable levels of p53 at baseline (Figure 5*A*). Cells were treated with CPM, and proliferation and apoptosis were assessed using soluble MTT and histone DNA-cleavage assays, respectively (Figure 5, *B* and *C*). Treatment with 4^{OH}-CPM (the active metabolite of CPM) resulted in effective growth inhibition in 10% serum (Figure 5*B*) or

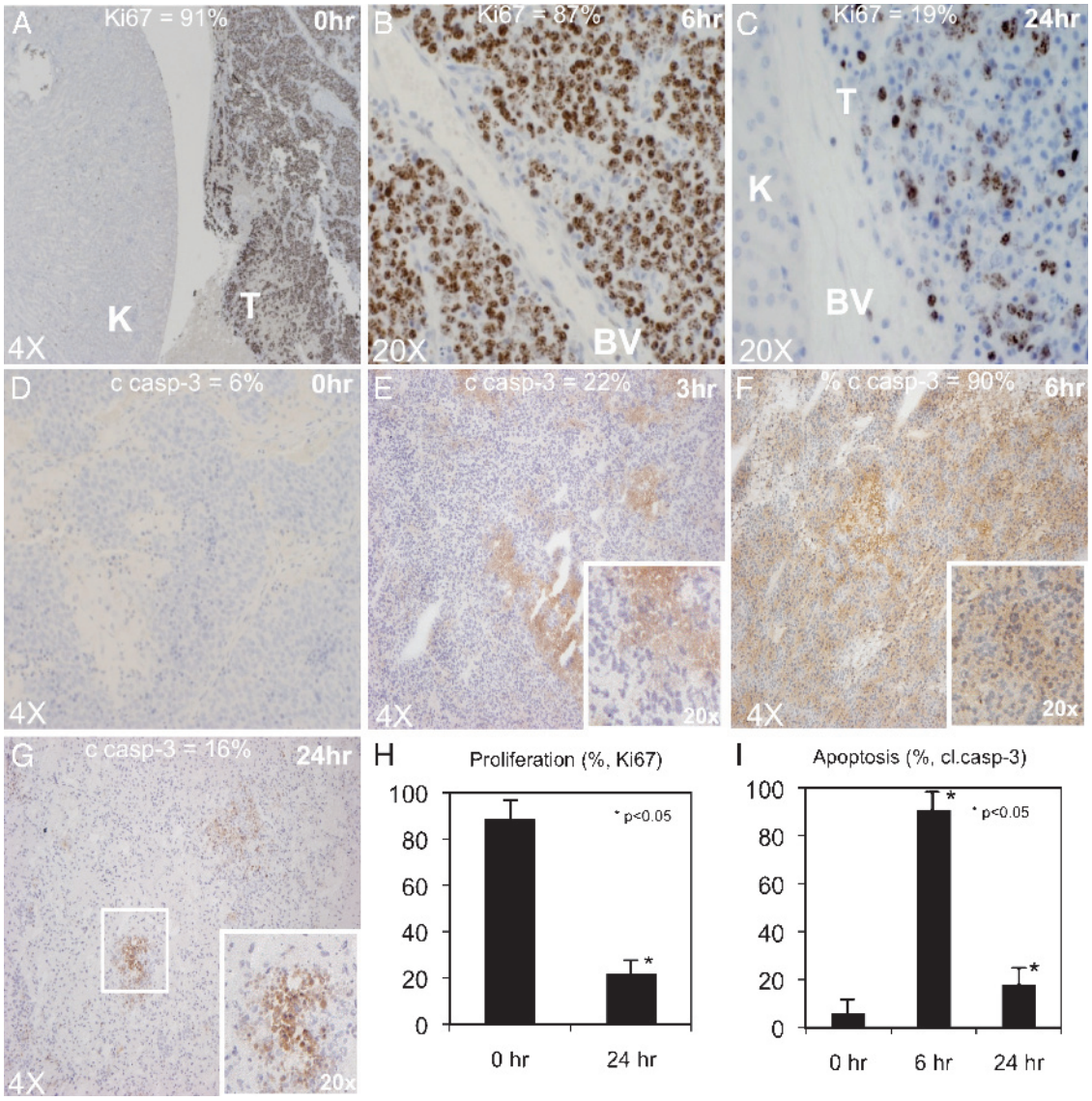

Figure 3. Proliferation blockade and apoptosis induction in CPM-treated murine neuroblastoma. Tumor-bearing animals were treated with CPM and killed, and tumors were fixed in paraffin. Immunoreactivity of Ki-67 (myb-1) in tumors (three per time point) treated for 0, 6, or 24 hours, respectively. *BV* indicates blood vessel; *K*, kidney; *T*, tumor. (A) Vehicle-treated tumors under low power (4×) show extensive Ki-67 immunoreactivity, reflecting the high proliferative index of such lesions. (B, C) Ki-67 staining is maximal at 6 hours and is notably diminished at 24 hours after CPM, highlighting the responsiveness of this tumor to the drug. (D–G) Cleaved caspase-3 immunostaining in formalin-fixed paraffin-embedded tumors is minimal in vehicle-treated tumors (D), but is rapidly induced at 3 hours (E), is maximal at 6 hours (F), and largely resolves by 24 hours (G) after CPM. Caspase-3 immunoreactivity at 24 hours is greatly reduced and is colocalized to regions of cellular breakdown and nuclear atypia (G). Insets: original magnification, ×20. *BV* indicates blood vessel; *K*, kidney; *T*, tumor. (H–I) Quantitation of Ki-67 staining (H) and cleaved caspase-3 staining (I) in the tumor sections shown in D–G at time points after CPM in five high-power fields per section from three separate tumor samples.

in low serum (data not shown). 4-Hydroxyperocyclophosphamide induced apoptosis in all cell lines, with increased apoptosis noted in the *MYCN*-amplified Kelly cell line (Figure 5*C*). These data are consistent with published findings that neuroblastoma cells amplified for *MYCN* are sensitized to the effects of cytotoxic chemotherapeutics [28]. Coincident with the induction of apoptosis by 4^{OH}-CPM, activation of p53 was still observed in such cells. We treated *MYCN*-amplified Kelly cells with 4^{OH}-CPM and cisplatin [*cis*-diamminedichloridoplatinum(II), CDDP], a bifunctional alkylator also used in frontline therapy for human neuroblastoma. In contrast to a lack of apoptosis observed in vehicle-treated spontaneous *in vivo* tumors, the vehicle-treated cultured cell lines displayed detectable basal apoptosis by immunoblot analysis. Analogous to the response observed in TH-*MYCN* tumors growing *in vivo*, p53 was strongly induced and phosphorylated in response to treatment with 4^{OH}-CPM, and maximal activity correlated with strong induction of caspase-3 cleavage at 6 hours (Figure 5*D*). Comparable activation was observed in response to CDDP, although with a slightly longer time course of p53 activation (Figure W3). Treatment of these cells with siRNA against p53 led to decreased levels of p53 total and phosphorylated proteins 6 hours after treatment with 4^{OH}-CPM, with a concomitant decrease in levels of the apoptotic marker cleaved caspase-3 (Figure W4). These results are consistent with previous findings indicating that the induction of p53 observed in murine

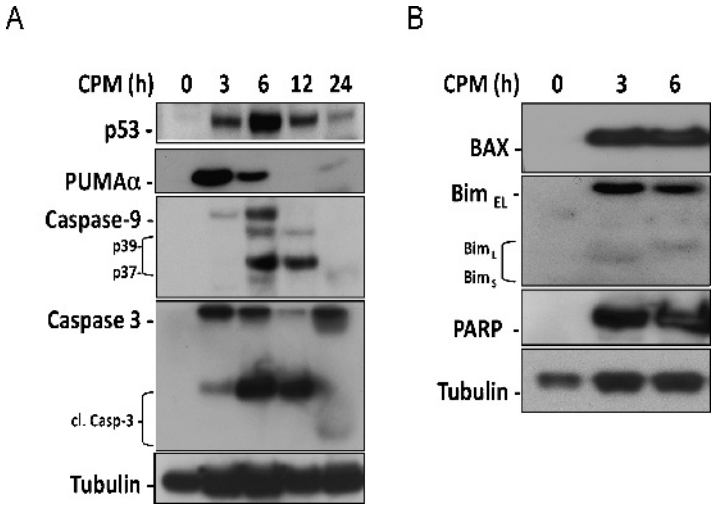

Figure 4. *In vivo* CPM treatment of murine neuroblastoma tumors induces p53 and p53 downstream targets. Tumors were harvested from transgene-positive animals at 0, 3, 6, 12, and 24 hours after therapy with CPM. Lysates were analyzed by immunoblot analysis for levels of apoptosis proteins. (A) Activation of the intrinsic (mitochondrial) apoptotic pathway occurs at 3 hours, with induction of p53 peaking at 6 hours after treatment. Activation of p53 was associated with cleavage of caspases-3 and -9, also peaking at 6 hours. PUMA was induced strongly, with a peak at 3 hours after treatment. (B) To assess the effect of CPM treatment on BH3-family proteins, lysates were probed for the activation of Bim and Bax. Rapid activations of Bax and Bim were coincident. These proteins are downstream targets of PUMA and c-*myc*, respectively, subject to p53 regulation of the chemotherapy-induced DNA damage response. Poly(ADP-ribose) polymerase cleavage indicates potent induction of apoptosis.

neuroblastoma is also evident in human tumors and that *MYCN*-amplified human neuroblastoma likely requires p53 for induction of apoptosis in response to cytotoxic chemotherapy.

Discussion

To our knowledge, this study is the first *in vivo* demonstration of the importance of intact p53 function to neuroblastoma tumor progression and chemoresponsiveness. In this *MYCN*-driven malignancy, the proliferative and apoptotic functions of *MYCN* are effectively uncoupled by functional suppression of p53-induced apoptosis (in the absence of *p53* mutation). Furthermore, any coexistent apoptotic defects required for transformation by *MYCN* are insufficient to block the apoptotic effect induced by cytotoxic chemotherapy. Mutation at *p53* is not generally observed in neuroblastoma tumors at diagnosis; however, epigenetic alterations (including silencing of caspase-8, increased levels of survivin and Bcl2, and cytoplasmic sequestration of p53) likely contribute to malignant progression [13,15,29]. Although these epigenetic abnormalities may underlie some relative chemoresistance, our data are consistent with observations in other tumor types suggesting that these abnormalities spare intrinsic mitochondrial apoptotic signaling, which can drive apoptosis in response to cytotoxic chemotherapy.

Cyclophosphamide, a first-line agent in children with newly diagnosed neuroblastoma, is active in murine neuroblastoma. Baseline apoptosis in spontaneously progressing TH-*MYCN* tumors is suppressed, and activation of such proteins is not detectable by immunoblot analysis, in contrast to observations in cultured neuroblastoma tumor cell lines *in vitro*. Cyclophosphamide treatment induces massive apoptosis proceeding through activation of p53 and the downstream Bcl-2-homology domain-3 (BH3) proteins, PUMA and Bim, indicating that apoptosis proceeds through mitochondrial-dependent pathways. Bax, a known effector of apoptosis in murine lymphoma, is also strongly induced [30]. PUMA, Bim, and Bax are all key effectors of p53-induced apoptosis, and alterations in PUMA expression modulate the phenotype of c-*myc*–driven tumors in genetically engineered mouse models of hematopoietic malignances [31]. PUMA complexes directly with p53, linking nuclear and cytosolic p53 fractions, and is required for induction of apoptosis by nuclear p53 [32]. Our observations argue that p53-driven apoptosis is functional but suppressed in spontaneous TH-*MYCN* tumors growing *in vivo*, that p53 and its effector PUMA are potential therapeutic targets in

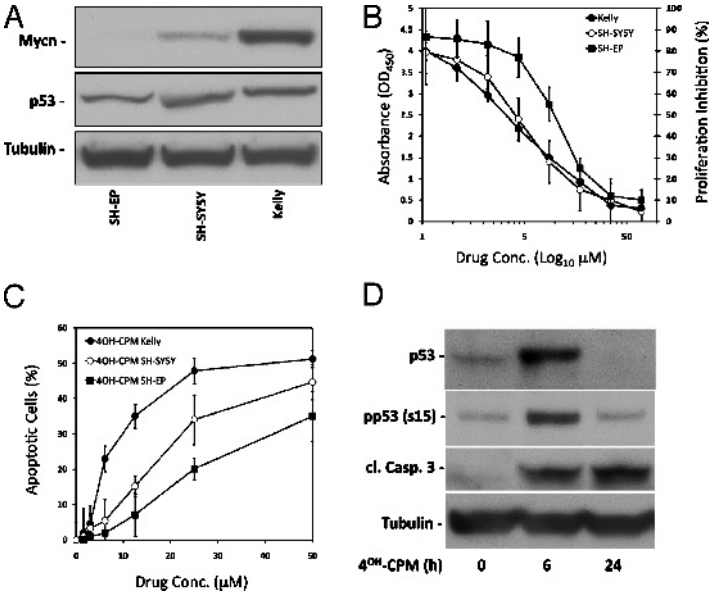

Figure 5. CPM induces apoptosis in *MYCN*-amplified neuroblastoma cell lines are sensitized to CPM-induced apoptosis and activate p53. Tumor cells were cultured in 10% FBS and treated with 4^{OH}-CPM at indicated doses for 24 hours. (A) Expression levels of Mycn and p53 protein in cultured cell lines SH-EP (*MYCN* diploid, no Mycn protein), SH-SY5Y (*MYCN* diploid, intermediate Mycn protein), and Kelly (*MYCN*-amplified, high Mycn protein) treated with 4^{OH}-CPM for 6 hours. (B) To assess the effect of CPM on proliferation, cells were analyzed at 24 hours by water-soluble tetrazolium (WST-1) assay. Kelly cells showed enhanced inhibition across the range of doses tested. Values represent means of triplicate measurements. (C) CPM induces apoptosis in human neuroblastoma cell lines. The same cells were treated for 24 hours, and apoptosis was assessed by nucleosomal DNA ELISA. Apoptosis was more readily evident in the *MYCN*-amplified Kelly cells. These data suggest that amplification of *MYCN* sensitizes human neuroblastoma cells to apoptosis induced by CPM and are consistent with observations that amplification of *MYCN* generally increases the susceptibility of cells to cytotoxic chemotherapy. (D) *MYCN*-amplified Kelly cells were treated with 20 μM 4^{OH}-CPM for 24 hours and analyzed by immunoblot analysis for levels of p53, phospho-p53 (S15), and caspase-3 proteins. Induction of caspase-3 cleavage occurs 6 hours after treatment with CPM coincident with maximal p53 induction and phosphorylation. This is consistent with the observations *in vivo* using TH-*MYCN* tumors.

neuroblastoma, and that agents that enhance the activity of p53 or PUMA may show efficacy in this disease.

Impaired p53 signaling likely enhances the oncogenic activity of *MYCN* in neuroblastoma [10–12,33,34] and probably contributes to relapse as additional (mutational) defects in this pathway are acquired with genotoxic therapy. These studies help to clarify observations in cell lines from human neuroblastoma, in which acquisition of mutations in *p53* occurred in cell lines established from relapsed tumors [11,24,33]. Collectively, our murine data are in agreement with human cell line data generated here and published by others, suggesting that cytotoxic drugs drive relapse by selecting for mutations in *p53* or in the p53 pathway. We are currently generating mice transgenic for TH-*MYCN* that are inducibly dysfunctional at *p53* and are backcrossing them into the penetrant 129/SvJ strain to determine the utility of these animals as a model for drug-resistant high-risk neuroblastoma at relapse.

Acknowledgments

The authors thank Scott Lowe, Gerard Evan, Jason Shohet, and members of the Weiss laboratory for useful discussions. The authors also thank Larry Donehower for supplying p53+/– mice, Eric Holland for supplying E_2F_1-luciferase mice, and Susan Ludeman for supplying the 4^{OH}-CPM.

References

[1] Maris JM and Matthay KK (1999). Molecular biology of neuroblastoma. *J Clin Oncol* **17**, 2264–2279.

[2] Matthay KK, Villablanca JG, Seeger RC, Stram DO, Harris RE, Ramsay NK, Swift P, Shimada H, Black CT, Brodeur GM, et al. (1999). Treatment of high-risk neuroblastoma with intensive chemotherapy, radiotherapy, autologous bone marrow transplantation, and 13-*cis*-retinoic acid. Children's Cancer Group. *N Engl J Med* **341**, 1165–1173.

[3] Schmidt ML, Lukens JN, Seeger RC, Brodeur GM, Shimada H, Gerbing RB, Stram DO, Perez C, Haase GM, and Matthay KK (2000). Biologic factors determine prognosis in infants with stage IV neuroblastoma: a prospective Children's Cancer Group Study. *J Clin Oncol* **18**, 1260–1268.

[4] Brodeur GM, Seeger RC, Schwab M, Varmus HE, and Bishop JM (1985). Amplification of N-*myc* sequences in primary human neuroblastomas: correlation with advanced disease stage. *Prog Clin Biol Res* **175**, 105–113.

[5] Seeger RC, Brodeur GM, Sather H, Dalton A, Siegel SE, Wong KY, and Hammond D (1985). Association of multiple copies of the N-*myc* oncogene with rapid progression of neuroblastomas. *N Engl J Med* **313**, 1111–1116.

[6] Fulda S, Lutz W, Schwab M, and Debatin KM (1999). MycN sensitizes neuroblastoma cells for drug-induced apoptosis. *Oncogene* **18**, 1479–1486.

[7] van Noesel MM, Pieters R, Voute PA, and Versteeg R (2003). The N-*myc* paradox: N-*myc* overexpression in neuroblastomas is associated with sensitivity as well as resistance to apoptosis. *Cancer Lett* **197**, 165–172.

[8] Lutz W, Stohr M, Schurmann J, Wenzel A, Lohr A, and Schwab M (1996). Conditional expression of N-*myc* in human neuroblastoma cells increases expression of alpha-prothymosin and ornithine decarboxylase and accelerates progression into S-phase early after mitogenic stimulation of quiescent cells. *Oncogene* **13**, 803–812.

[9] Keshelava N, Seeger RC, and Reynolds CP (1997). Drug resistance in human neuroblastoma cell lines correlates with clinical therapy. *Eur J Cancer* **33**, 2002–2006.

[10] Keshelava N, Seeger RC, Groshen S, and Reynolds CP (1998). Drug resistance patterns of human neuroblastoma cell lines derived from patients at different phases of therapy. *Cancer Res* **58**, 5396–5405.

[11] Carr J, Bell E, Pearson AD, Kees UR, Beris H, Lunec J, and Tweddle DA (2006). Increased frequency of aberrations in the p53/MDM2/p14(ARF) pathway in neuroblastoma cell lines established at relapse. *Cancer Res* **66**, 2138–2145.

[12] Tweddle DA, Malcolm AJ, Bown N, Pearson AD, and Lunec J (2001). Evidence for the development of *p53* mutations after cytotoxic therapy in a neuroblastoma cell line. *Cancer Res* **61**, 8–13.

[13] Islam A, Kageyama H, Takada N, Kawamoto T, Takayasu H, Isogai E, Ohira M, Hashizume K, Kobayashi H, Kaneko Y, et al. (2000). High expression of survivin, mapped to 17q25, is significantly associated with poor prognostic factors and promotes cell survival in human neuroblastoma. *Oncogene* **19**, 617–623.

[14] Eggert A, Grotzer MA, Zuzak TJ, Wiewrodt BR, Ikegaki N, and Brodeur GM (2000). Resistance to TRAIL-induced apoptosis in neuroblastoma cells correlates with a loss of caspase-8 expression. *Med Pediatr Oncol* **35**, 603–607.

[15] Teitz T, Wei T, Valentine MB, Vanin EF, Grenet J, Valentine VA, Behm FG, Look AT, Lahti JM, and Kidd VJ (2000). Caspase 8 is deleted or silenced preferentially in childhood neuroblastomas with amplification of *MYCN*. *Nat Med* **6**, 529–535.

[16] Castle VP, Heidelberger KP, Bromberg J, Ou X, Dole M, and Nunez G (1993). Expression of the apoptosis-suppressing protein bcl-2, in neuroblastoma is associated with unfavorable histology and N-*myc* amplification. *Am J Pathol* **143**, 1543–1550.

[17] Mora J, Cheung NK, and Gerald WL (2001). Genetic heterogeneity and clonal evolution in neuroblastoma. *Br J Cancer* **85**, 182–189.

[18] Teitz T, Lahti JM, and Kidd VJ (2001). Aggressive childhood neuroblastomas do not express caspase-8: an important component of programmed cell death. *J Mol Med* **79**, 428–436.

[19] Norris MD, Bordow SB, Haber PS, Marshall GM, Kavallaris M, Madafiglio J, Cohn SL, Salwen H, Schmidt ML, Hipfner DR, et al. (1997). Evidence that the *MYCN* oncogene regulates *MRP* gene expression in neuroblastoma. *Eur J Cancer* **33**, 1911–1916.

[20] Weiss WA, Aldape K, Mohapatra G, Feuerstein BG, and Bishop JM (1997). Targeted expression of *MYCN* causes neuroblastoma in transgenic mice. *EMBO J* **16**, 2985–2995.

[21] Norris MD, Burkhart CA, Marshall GM, Weiss WA, and Haber M (2000). Expression of N-*myc* and *MRP* genes and their relationship to N-*myc* gene dosage and tumor formation in a murine neuroblastoma model. *Med Pediatr Oncol* **35**, 585–589.

[22] Maris JM, Weiss MJ, Guo C, Gerbing RB, Stram DO, White PS, Hogarty MH, Sulman EP, Thompson PM, Lukens JN, et al. (2000). Loss of heterozygosity at 1p36 independently predicts for disease progression, but not decreased overall survival probability, in neuroblastoma patients: a Children's Cancer Group Study. *J Clin Oncol* **18**, 1888–1899.

[23] Keshelava N, Zuo JJ, Waidyaratne NS, Triche TJ, and Reynolds CP (2000). *p53* mutations and loss of p53 function confer multidrug resistance in neuroblastoma. *Med Pediatr Oncol* **35**, 563–568.

[24] Keshelava N, Zuo JJ, Chen P, Waidyaratne SN, Luna MC, Gomer CJ, Triche TJ, and Reynolds CP (2001). Loss of p53 function confers high-level multidrug resistance in neuroblastoma cell lines. *Cancer Res* **61**, 6185–6193.

[25] Donehower LA, Harvey M, Slagle BL, McArthur MJ, Montgomery CA Jr, Butel JS, and Bradley A (1992). Mice deficient for p53 are developmentally normal but susceptible to spontaneous tumours. *Nature* **356**, 215–221.

[26] Momota H and Holland EC (2005). Bioluminescence technology for imaging cell proliferation. *Curr Opin Biotechnol* **16**, 681–686.

[27] Jeffers JR, Parganas E, Lee Y, Yang C, Wang J, Brennan J, MacLean KH, Han J, Chittenden T, Ihle JN, et al. (2003). Puma is an essential mediator of p53-dependent and -independent apoptotic pathways. *Cancer Cell* **4**, 321–328.

[28] Fulda S, Lutz W, Schwab M, and Debatin KM (2000). MycN sensitizes neuroblastoma cells for drug-triggered apoptosis. *Med Pediatr Oncol* **35**, 582–584.

[29] Reed JC, Meister L, Tanaka S, Cuddy M, Yum S, Geyer C, and Pleasure D (1991). Differential expression of *bcl2* protooncogene in neuroblastoma and other human tumor cell lines of neural origin. *Cancer Res* **51**, 6529–6538.

[30] Dansen F, Whitfield J, Rostker F, Brown-Swigart L, and Evan G (2006). Specific requirement for Bax, not Bak, in Myc-induced apoptosis and tumor suppression *in vivo*. *J Biol Chem* **281**, 10890–10895.

[31] Hemann MT, Zilfou JT, Zhao Z, Burgess DJ, Hannon GJ, and Lowe SW (2004). Suppression of tumorigenesis by the p53 target PUMA. *Proc Natl Acad Sci USA* **101**, 9333–9338.

[32] Chipuk JE, Bouchier-Hayes L, Kuwana T, Newmeyer DD, and Green DR (2005). PUMA couples the nuclear and cytoplasmic proapoptotic function of p53. *Science* **309**, 1732–1735.

[33] Xue C, Haber M, Flemming C, Marshall GM, Lock RB, Mackenzie KL, Gurova KV, Norris MD, and Gudkov AV (2007). p53 determines multidrug sensitivity of childhood neuroblastoma. *Cancer Res* **67**, 10351–10360.

[34] Armstrong MB, Bian X, Liu Y, Subramanian C, Ratanaproeksa AB, Shao F, Yu VC, Kwok RP, Opipari AW, and Castle VP (2006 Nov). Signaling from p53 to NF-kappa B determines the chemotherapy responsiveness of neuroblastoma. *Neoplasia* **8** (11), 964–974.

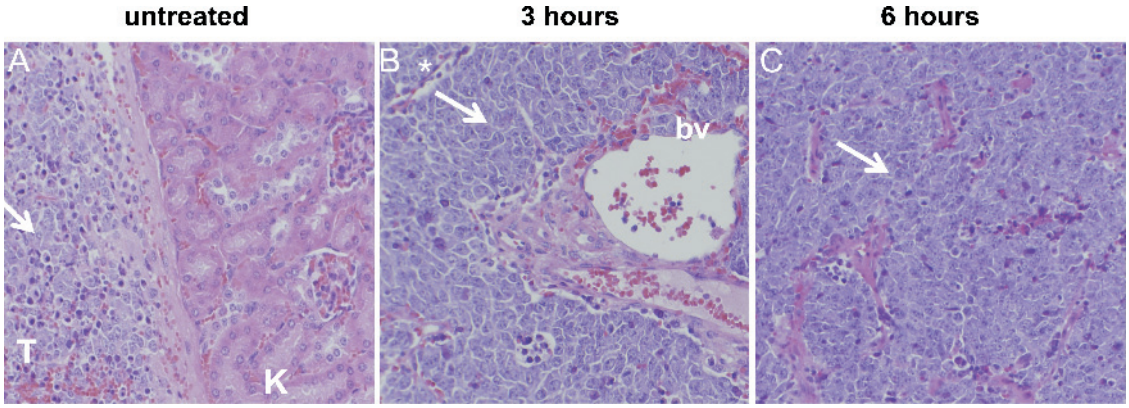

Figure W1. Morphology of TH-*MYCN* neuroblastoma tumors treated with CPM. (A–C) Animals were treated intraperitoneally with 150 mg/kg CPM for 0, 3, and 6 hours, and tumors were harvested, fixed in formalin, embedded in paraffin, and sectioned for hematoxylin and eosin staining. No major structural changes were observed, and cellular morphology of neuroblasts (arrows) was unaltered. *BV* indicates blood vessel; *K*, kidney; *T*, tumor.

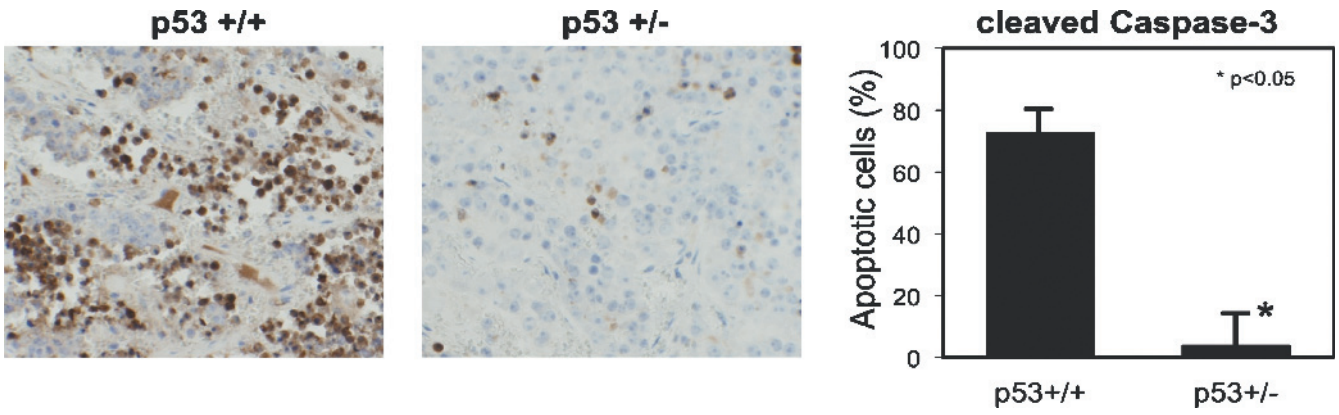

Figure W2. Apoptosis in p53+/− TH-*MYCN* tumors in response to CPM administered *in vivo*. In contrast to p53 +/+ TH-*MYCN* tumors, which show potent activation of caspase-3 cleavage 6 hours after treatment with CPM (150 mg/kg given intraperitoneally), p53+/− tumors fail to show significant induction of caspase-3 staining after treatment (representative staining from a cohort of three replicate tumors per group). Caspase-3 cleavage is quantitated in the right panel. No significant changes in caspase-3 staining were seen between vehicle-treated p53+/− and p53+/+ tumors (data not shown).

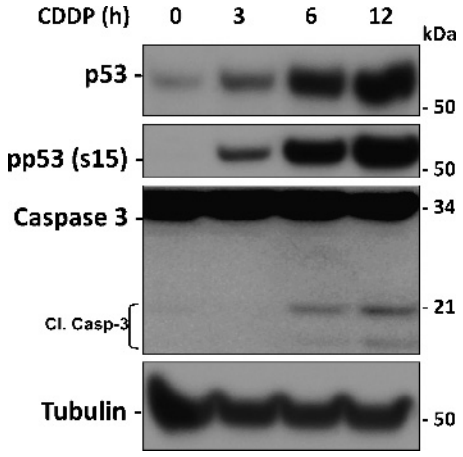

Figure W3. Response of human *MYCN*-amplified neuroblastoma cells to cisplatin (CDDP). Kelly cells were cultured and treated as in Figure 4, using 15 μM cisplatin, and were immunoblotted for p53, phospho-p53 (Ser 15), and caspase-3. Induction and activation of p53 is observed commencing at 3 hours after CDDP, with prolonged activation until 12 hours corresponding to the activation of caspase-3 cleavage beginning at 6 hours.

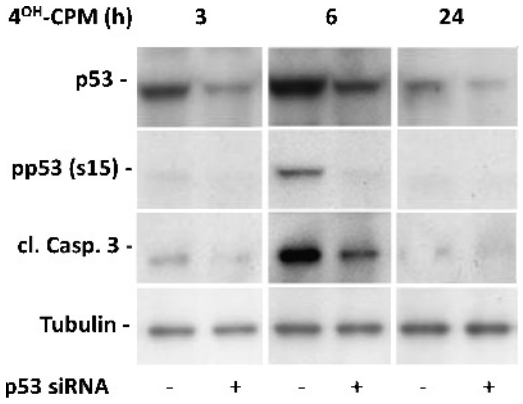

Figure W4. Inhibition of p53 using RNA interference. *MYCN*-amplified Kelly cells were transiently transfected with p53 siRNA. Inhibition of p53 reduces p53 activation and phosphorylation of p53 (Ser 15) at 6 hours, with consequent reduction of caspase-3 cleavage, implying a requirement for p53 function in the apoptotic response of these cells to chemotherapy.